INTERNATIONAL JOURNAL OF IMMUNOPATHOLOGY AND PHARMACOLOGY Vol. 20, no. 4, 685-695 (2007)

METALLIC NANOPARTICLES EXHIBIT PARADOXICAL EFFECTS ON OXIDATIVE STRESS AND PRO-INFLAMMATORY RESPONSE IN ENDOTHELIAL CELLS *IN VITRO*

K. PETERS, R.E. UNGER, A.M. GATTI[1], E. SABBIONI[2], R. TSARYK and C.J. KIRKPATRICK

Institute of Pathology, Johannes Gutenberg University, Mainz, Germany; [1]INFM, Laboratory of Biomaterials, Department of Neurosciences, University of Modena and Reggio Emilia, Modena; [2]European Commission, Institute for Health and Consumer Protection, Joint Research Centre, Ispra, Italy

Received February 20, 2007 – Accepted July 27, 2007

Particulate matter is associated with different human diseases affecting organs such as the respiratory and cardiovascular systems. Very small particles (nanoparticles) have been shown to be rapidly internalized into the body. Since the sites of internalization and the location of the detected particles are often far apart, a distribution via the blood stream must have occurred. Thus, endothelial cells, which line the inner surface of blood vessels, must have had direct contact with the particles. In this study we tested the effects of metallic nanoparticles (Co and Ni) on oxidative stress and pro-inflammatory response in human endothelial cells *in vitro*. Exposure to both nanoparticle types led to a concentration-dependent cytotoxic effect. However, the effects on oxidative stress and pro-inflammatory response differed dramatically. Due to the nanoparticle-induced effects, a comparison between metallic nanoparticle- and metal ion-treatment with the corresponding ions was made. Again, divergent effects of nanoparticles compared with the ions were observed, thus indicating differences in the signaling pathways induced by these compounds. These paradoxical responses to different metallic nanoparticles and ions demonstrate the complexity of nanoparticle-induced effects and suggest the need to design new strategies for nanoparticle toxicology.

The human body is exposed to many types of particles during its lifetime. These particles can be of natural origin or they can develop as (by-)products of industrial processes, and technical or pharmaceutical engineering. These particles vary considerably in composition, size, shape, surface property and habitat. Depending on these characteristics, the internalization of particles and their dissemination within the body is variable and may take place by ingestion (from polluted food or food additives) (1), inhalation (smoking, diesel soot, medical aerosols), via the skin (e.g. cosmetics, pharmaceutics), implantation (e.g. wear from implants) (2), and also injection (e.g. drug delivery and cancer therapy) (3).

Particulate air pollution is associated with enhanced mortality from respiratory and cardiovascular diseases (4). Among the most abundant air pollutants in urban areas is particulate matter with a mean diameter of ≤ 10 µm. Particles with very low sizes (especially those with sizes below 100 nm, called ultrafine particles or nanoparticles) have been shown to induce more severe effects

Key words: nanoparticles, metal ions, endothelial cells, inflammation, cytotoxicity, in vitro, oxidative stress, ROS, nanotoxicology

Mailing address: Dr Kirsten Peters,
Junior Research Group "Bone Regeneration,
Department of Cell Biology,
Biomedical Research Center (BMFZ),
Schillingallee 69, 18057 Rostock, Germany
Tel.: ++49 381 494 7757 Fax: ++49 381 494 7778
e-mail: kirsten.peters@med.uni-rostock.de

0394-6320 (2007)

than larger particles (5-6). A trigger for this higher effectiveness is the surface area/volume-ratio, which increases exponentially with decreasing particle sizes leading to increased surface reactivity. This increased surface reactivity could lead to greater biological activity per given mass compared to larger particles, which in turn might have effects on, for example, the particle internalization into tissues, cells and organelles, toxicity, or the induction of oxidative stress (3, 7). Oxidative stress describes a condition in which the generation of reactive oxygen species (ROS) exceeds the system's ROS-defense mechanisms. Oxidative stress affects many cellular functions by damaging nucleic acids, oxidizing proteins and causing lipid peroxidation. It has been well established that oxidative stress is associated with several human pathological conditions, including cancer, cardiovascular and autoimmune diseases (8).

The internalization of nanoparticles into the body's tissues appears to be easy due to their minute size. This is shown by animal studies where inhaled nanoparticles were translocated into lung-associated lymph nodes and the brain (9-10). As the sites of internalization of nanoparticles (food, air, etc.) and the location of the detected particles are generally far apart, a distribution via the blood stream must have occurred. Thus, endothelial cells (EC), which line the inner surface of blood vessels, must have had direct contact with the particles. In animal experiments it was shown that inhaled particles could be detected within capillaries and EC (11) which could lead to systemic microvascular dysfunction and inflammation (12).

EC are important in inflammation and wound healing. Upon pro-inflammatory stimulation adhesion molecules are expressed on the EC surface, thus mediating leukocyte attachment (e.g. E-selectin and intercellular adhesion molecule-1/ICAM-1). Furthermore, EC are able to release cytokines, such as interleukin-8 (IL-8, a key factor in neutrophil chemotaxis). The activation of IL-8, E-selectin and ICAM-1 is regulated by the same transcription factors NF-κB (nuclear factor-κB) and AP-1 (activator protein-1) (13-15). These features contribute to the pro-inflammatory endothelial phenotype permitting the transmigration of leukocytes from the blood into the perivascular space. Both, NF-κB and AP-1 are also known to be activated by oxidative stress (16).

To date little is known about the effects of nanoparticles on EC functions. Therefore, the subject matter of this study was to test the effects of metallic nanoparticles on human EC *in vitro*. Metallic nanoparticles of Co and Ni were examined with respect to cellular internalization and their influence on cell viability, the induction of oxidative stress and a pro-inflammatory endothelial phenotype. Moreover, a comparison between metallic nanoparticle- and metal ion-treatment with the corresponding ions (Co^{2+}, Ni^{2+}) was made.

MATERIALS AND METHODS

All chemicals were obtained from Sigma (Germany) if not otherwise indicated.

Cell culture

Human dermal microvascular EC (HDMEC) were isolated from juvenile foreskin as described before (17) and cultured in *Endothelial Cell Basal Medium MV* (PromoCell, Germany) supplemented with 15% fetal calf serum (Invitrogen, Germany), basic fibroblast growth factor (bFGF, 2.5 ng/ml), sodium heparin (10 µg/ml), Penicillin/Streptomycin (10,000 units penicillin/ml, 10,000 µg streptomycin sulfate/ml, Invitrogen), cultivated in a humidified atmosphere at 37°C (5% CO_2) and used after four subcultivation steps.

Particles

The mean size of Co particles was 28 nm with 99.8% purity (Nanoamor, USA). The mean particle size of Ni particles was 62 nm with more than 99% purity (Nanoamor, USA). The particles were added to the cell culture medium and tested at three different concentrations (0.5, 5, and 50 µg/ml culture medium).

Transmission electron microscopy (TEM)

Cells were seeded onto fibronectin-coated Thermanox coverslips (Nunc, Germany). Exposure to particles was performed two days after seeding (50 µg particles/ml). After 48 h incubation cells were fixed in cacodylate-buffered glutaraldehyde (2.5 %) and embedded in Agar100 (Plano, Germany). Ultrathin sections were made with the Ultracut E microtome (Leica, Germany) and stained with uranylacetate and lead citrate. TEM was performed with Phillips 410 EM (Phillips, Germany).

Quantification of cell number by crystal violet

Crystal violet (N-hexamethylpararosaniline) is a

basic dye, which stains cell nuclei (18). Gillies et al. used this dye characteristic to develop a sensitive method of quantification of relative cell number (19). The crystal violet assay was performed in a microplate format as described previously (20). Endothelial cells built up a monolayer where the cells directly detach from the growth substrate during cell death. The presence of transition metal ions makes other cytotoxicity tests, like the LDH-release assay that depend on a dye reaction, inoperative.

Quantification of IL-8 and MCP-1 release

Cells were seeded onto fibronectin-coated microtiter plates (11,000 cells/well), grown to confluence and exposed to particles (0.5, 5, and 50 μg/ml culture medium) and TNFα (tumor necrosis factor-α, 300 U/ml; pro-inflammatory control), respectively. Cell culture supernatants were collected 24 h after substance or particle exposure. IL-8 in supernatants was assayed using human IL-8 immunoassay/ELISA (Hiss Diagnostics, Germany) according to the manufacturer's instructions. MCP-1 (monocyte chemoattractant protein-1) in supernatants was quantified by an ELISA-kit from R&D Systems/Germany (human MCP-1 DuoSet) according to the manufacturer's instructions.

Quantification of ICAM-1 protein

This antigen is up-regulated in inflammatory-stimulated EC and can be detected by using an enzyme-linked immunoassay based on a peroxidase staining reaction and the subsequent dye quantification by a microplate reader. Therefore, cells were seeded onto fibronectin-coated 96-well microtiter plates (11,000 cells/well) and grown to confluence. Afterwards cells were subjected to specific cell culture conditions (different particle- and metal ion concentrations and TNFα as a positive control, 300 U/ml) and cultivated for an additional 24 h. The cells were fixed with methanol/ethanol (2:1, 15 min, room temperature) and permeabilized with PBS-buffered 0.1% Triton X-100 (5 min, room temperature).

ICAM-1 was detected with mouse-anti human ICAM-1-antibody (Bender MedSystems, Germany, monoclonal IgG1 mouse antibody). The secondary antibody was a biotinylated goat-anti mouse-antibody (Amersham, Germany). Afterwards the streptavidin-horseradish peroxidase conjugate was added (Amersham). The staining reaction was performed by addition of the peroxidase-substrate (o-phenylen-diamin-dihydrochloride, R&D-Systems) for 15 min at 37°C. The staining reaction was stopped with 3 M HCl. Light extinction was determined with a microtiter plate spectrophotometer (ThermoLab Systems, Germany) at 492 nm.

Analysis of reactive oxygen species (ROS) by DCDHF-DA

2′,7′-dichlorodihydrofluorescein diacetate (DCDHF-DA) is commonly used to detect the generation of ROS, since cellular internalization and oxidation lead to the development of a fluorescent product (2′,7′-dichlorofluorescein, DCF) (21). Therefore HDMEC were seeded onto fibronectin-coated 96-well microtiter plates (11,000 cells/well) and grown to confluence. Before treatment HDMEC were incubated for 45 min with medium containing 100 μM DCDHF-DA (Alexis, Germany). Subsequently, the medium was changed and the cells were treated with the Co and Ni nanoparticles and the metal ion salts in different concentrations (mentioned in the text). In the following, the fluorescence of the cells was analyzed by a microplate fluorescence reader (Tecan) after 30 min, 1 h, 4 h and (partially) 24 h. The excitation of fluorescence was achieved with a 485 nm filter, emission was by 535 nm. Analysis took place by the XFluor4 software (Tecan).

Quantification of reduced glutathione (GSH)

HDMEC were seeded in 24-well plates (100,000 cells/well) and grown to confluence (after 2 days). The cells were then treated with the compounds (0.5 mM H_2O_2 as positive control, 25 and 50 μg/ml Co and Ni particles, and 0.5 and 1 mM $CoCl_2$/$NiCl_2$). After 24 h the cells were lysed with 100 μl lysis-buffer/well for 10 min at room temperature while stirring (chilled lysis-buffer: 20 mM Tris-HCl, pH 7.5; 150 mM NaCl, 1 mM EDTA, 1 mM EGTA, 1% Triton X-100). The lysates were centrifuged (4°C, 10 min, 15.000 g) and transferred into a 96-well-flat bottom-plate. Afterwards, glutathione transferase from equine liver (1 U) and 0.1 mM monochlorobimane (Fluka, Germany) were added (solved in lysis-buffer, see above). Also standards for GSH were tested (5, 10, 25 μM). All samples were incubated at 37°C for 30 min. The fluorescence was then analyzed by a microplate fluorescence reader (Tecan, Germany). The excitation of fluorescence was achieved with a 395 nm filter, emission was by 485 nm. Analysis took place by the XFluor4 software (Tecan). The glutathione amounts were normalized against the total protein amount. The protein quantitation was performed by the Bradford protein-assay (22).

Statistical analysis

All results are shown as means ± standard deviations (SD). Each individual experiment was done in triplicate. Statistical analysis was carried out with Microsoft excel software. According to the results of variance ratio analysis (F-test $p<0.05$) an unpaired t-test for either homoscedastic of heteroscedastic variances was performed ($p<0.05$).

RESULTS

Particle internalization

Ultrastructural studies from perpendicular sections

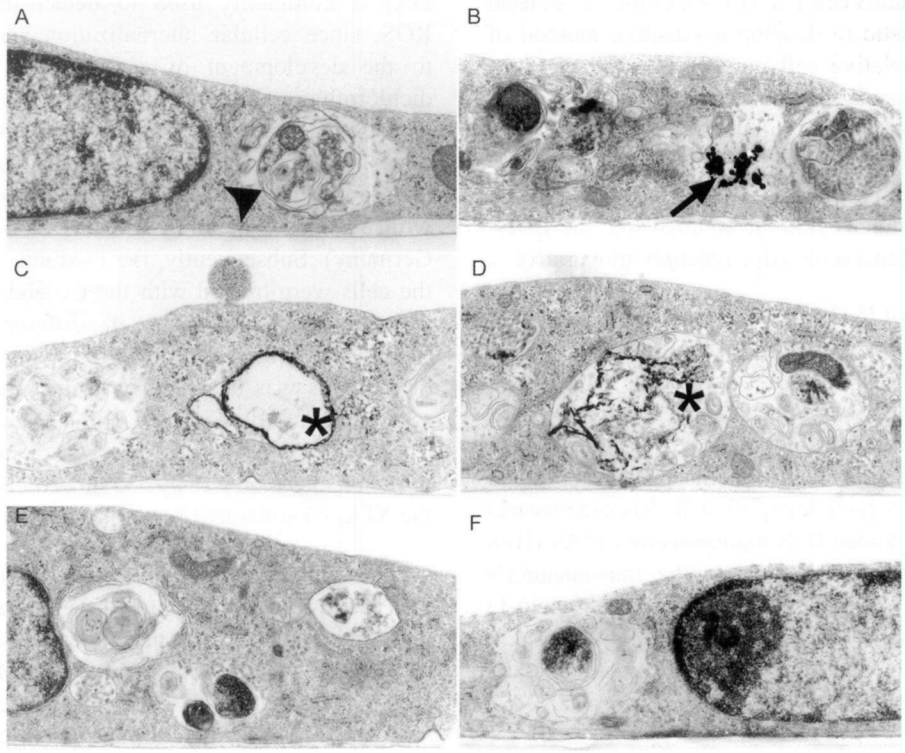

Fig. 1. *Perpendicular sections of HDMEC monolayers. a) non-treated HDMEC (control, arrowhead: autophagic vacuole) and HDMEC exposed to b) Ni particles (arrow: vacuole-stored particle accumulation), c/d) Co particles (asterisks: annular-shaped particle formations), e) 1 mM Co^{2+}, f) 1 mM Ni^{2+} (TEM, magnification 26,000 x).*

of endothelial cell monolayers with TEM demonstrated that the cytoplasm of the untreated HDMEC possessed numerous vacuoles. Many vacuoles contained cellular debris, such as membrane materials, which was due to the autophagic function of these vacuoles (Fig. 1a, untreated control, arrowhead: autophagic vacuole, also called secondary lysosome). When HDMEC were exposed to Ni and Co nanoparticles, these compounds were internalized (Fig. 1b: Ni particles, Fig. 1c/d: Co particles). The particles were localized within the cytoplasmic vacuoles, which partially contained additional cellular debris. Whereas internalized Ni nanoparticles were arranged in clusters (Fig. 1b, arrow), Co nanoparticles were arranged as annular-shaped, optically interconnected formations (asterisks), which lined the inner surface of the vacuoles (Fig. 1c) and were partially distributed without contact with the vacuolar membrane (Fig. 1d).

The possible corrosion products of commercially pure Co and Ni nanoparticles are their ions (mainly divalent ions). Therefore, we compared the effects of the respective ions in concentrations that were equivalent to the molarity of the utilized particles (e.g. 50 µg Co particles per ml corresponded to 0.85 mM Co^{2+}, 25 µg/ml corresponded to 0.42 mM and 10 µg/ml to 0.17 mM; the calculations depending on the assumption that pure Co and Ni particles were present and were therefore only an approximation). The treatment with high concentrations (1 mM) of both, Co^{2+} and Ni^{2+} ions did not induce striking changes to the ultrastructure of EC (Fig. 1e: Co^{2+}; Fig. 1f: Ni^{2+}).

Cytotoxicity

The exposure of both Co and Ni nanoparticles to confluent endothelial cultures induced a concentration-dependent reduction of endothelial cell number within 24 h (Fig. 2a: Co particles, Fig. 2b: Ni particles, detected by nuclear staining with crystal violet). This was due to a cytotoxic effect induced by the nanoparticles. The highest tested Co nanoparticle concentration (50 µg/ml medium)

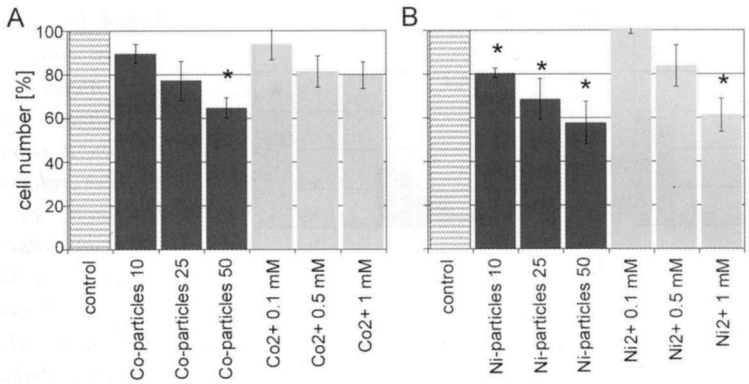

Fig. 2. *Cytotoxicity of nanoparticles and metal ions in HDMEC, a) Co compounds (Co nanoparticles and $CoCl_2$), b) Ni compounds (Ni nanoparticles and $NiCl_2$, crystal violet staining, 24 h exposure, particle amounts are given in µg/ml, untreated control set as 100%; n=4, means ± SDs, significantly different from control: *p<0.01).*

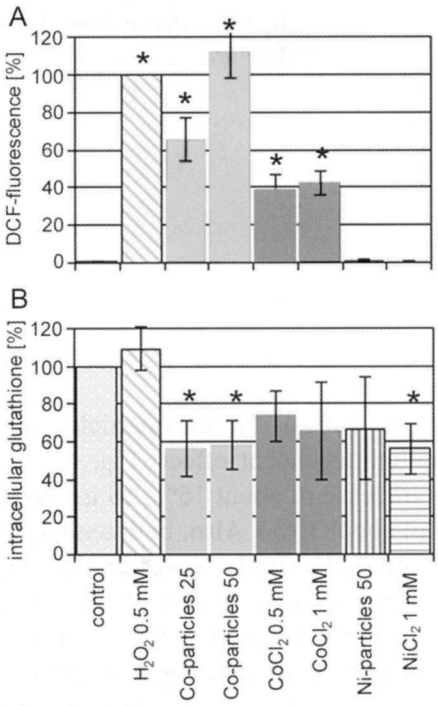

Fig. 3. *Evaluation of oxidative stress by detection of ROS and analysis of GSH a) DCF-fluorescence (4 h exposure), b) GSH-levels (24 h exposure, particle amounts are given in µg/ml, untreated control set as 100%; n=4, means ± SDs, significantly different from control: *p<0.01).*

induced a reduction of approximately 35% and the same concentration of Ni particles induced a more than 40% reduction of cell number. Interestingly, the exposure to the respective ions induced smaller effects (Fig. 2a: Co^{2+} ions, Fig. 2b: Ni^{2+} ions). Here, the exposure to the highest Co^{2+}-concentration tested (1 mM, i.e. a higher concentration than the approximate concentration of cobalt in nanoparticle formulation that is 0.85 mM) induced a reduction of cell number of about 20%, the highest Ni^{2+} concentration induced a reduction of about 40%.

Oxidative stress

One direct indication for the acute development of ROS is given by the utilization of DCDHF-DA; the oxidation of this molecule by ROS leading to the conversion to the fluorescent product DCF. The exposure of HDMEC to the different compounds tested revealed a heterogeneous pattern of development of DCF-fluorescence after 4 h (Fig. 3a). Co nanoparticles induced a strong, concentration-dependent increase in fluorescence (25 µg/ml led to ca. 65% of the fluorescence of the positive control H_2O_2, 50 µg/ml induced an increase of about 110% compared to the positive control), whereas $CoCl_2$ induced a concentration-independent DCF-fluorescence in HDMEC (both $CoCl_2$-concentrations induced a fluorescence of about 40% in comparison to the positive control). Interestingly, both Ni compounds (nanoparticles and chloride salt) did not induce DCF-fluorescence. To exclude that Ni compounds interfered with the DCF-fluorescence by ROS, H_2O_2 was added in the Ni containing experiments. Since full fluorescence was achieved with the combination of H_2O_2 and Ni, it can be concluded that Ni compounds did not

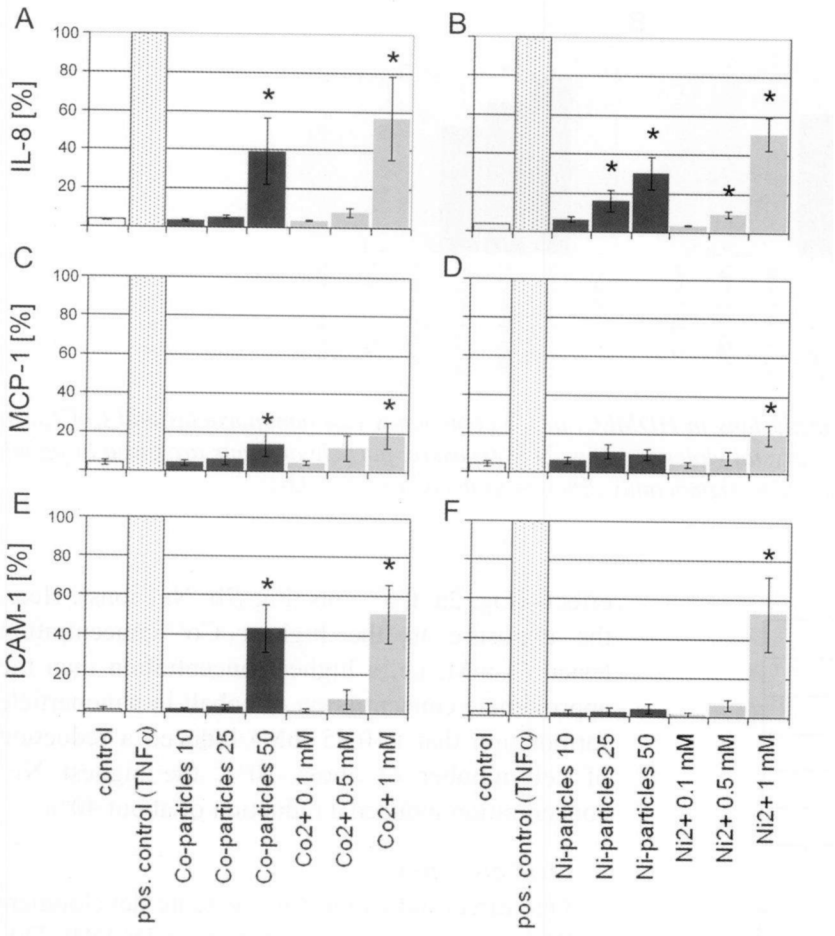

Fig. 4. *Detection of pro-inflammatory effects induced by nanoparticle and metal ion exposure, a) IL-8 release after Co compound-treatment (nanoparticles and ions), b) IL-8 release after Ni compound treatment, c) MCP-1 release after Co compound treatment, d) MCP-1 release after Ni compound treatment, e) ICAM-1 protein expression after Co compound treatment, f) ICAM-1 after Ni compound treatment (TNFα-stimulated cells serve as positive control and set as 100%, particle amounts are given in μg/ml, n=4, means ± SDs, significantly different from untreated control: *p<0.01; 24 h exposure, IL-8-data are reprinted with kind permission from Wiley VCH (46).*

interfere with the fluorescence development (data not shown).

An indirect measure for persistent oxidative stress is the cellular depletion of reduced glutathione (GSH). GSH is part of a redox buffer that is converted to glutathione disulfide under oxidative conditions. 24 h exposure to Co particles and $CoCl_2$ induced a reduction of GSH (Fig. 3b; both Co particle concentrations induced a similar reduction of more than 40%, $CoCl_2$ induced a reduction of about 30%). Also, both Ni compounds induced a distinct GSH depletion (Fig. 3b, reduction of about 40%).

Pro-inflammatory effects

IL-8 release by EC was stimulated by a 24 h exposure to high amounts of Co and Ni nanoparticles (Fig. 4a/b). Whereas for Co nanoparticles only the highest concentration tested (50 μg/ml) induced an increase of about 40% in comparison to the positive control (Fig. 4a, positive control: TNFα-stimulated cells, set as 100%), Ni nanoparticles induced a concentration-dependent effect (Fig. 4b; 25 μg/ml led to an increase of about 15%; 50 μg/ml led to an increase of about 30%). Also, both ion species, Co^{2+} and Ni^{2+}, induced a similar concentration-dependent IL-8 release (Fig. 4a/b, 1 mM of Co^{2+} induced an increase of approximately 55%, 1 mM of Ni^{2+} induced an increase of approximately 50%).

The release of the pro-inflammatory chemokine MCP-1 by metallic nanoparticles and their respective divalent ions was not as pronounced after 24 h. In fact, the exposure to Co nanoparticles and Co^{2+} ions induced a concentration-dependent increase (Fig. 4c). However, the highest concentrations tested (i.e. 50 μg/ml for the nanoparticles and 1 mM Co^{2+}) induced a slight increase of 15% for Co nanoparticles and of 20% increase for Co^{2+} ions, respectively. Ni nanoparticles did not induce a consistent effect in MCP-1 release, in that non-significant, not concentration-dependent changes in

the release of MCP-1 were detectable (Fig. 4d). Ni^{2+} ions, in contrast, induced a concentration-dependent increase (Fig. 4d, 1 mM Ni^{2+} induced a 20% increase in MCP-1 release).

The exposure of Co nanoparticles to EC resulted in an increase of the pro-inflammatory adhesion molecule ICAM-1. Significant ICAM-1 expression was detectable only at high Co particle amounts (i.e. 50 μg/ml, approx. 40% increase in comparison to the positive control) (Fig. 4e). The highest Co^{2+} ion concentrations (0.5 and 1 mM) induced a concentration-dependent increase in ICAM-1 protein expression (approx. 50% of the positive control by 1 mM Co^{2+}). In contrast to Co nanoparticles, Ni nanoparticles did not induce a significant increase in ICAM-1 expression (Fig. 4f). Interestingly, Ni^{2+} ions induced a similar increase in ICAM-1 expression as Co^{2+} ions (Fig. 4f).

DISCUSSION

Particle internalization

Human EC possess the capacity for the internalization of nanoparticles (23-25). In this study we showed that the nanoparticles tested were taken up by the EC and stored primarily in vacuoles. It is known that EC are able to internalize particles by different mechanisms. A large portion of the EC population possesses a vesicular system that is called the vesiculo-vacuolar organelle (VVO) that other cells do not have with this specificity. The VVO together with specific invaginations of the plasma membrane, the caveolae are involved in the regulated transendothelial cell passage of macromolecules and particles (26). This method of particle internalization might be specific for EC, since such a distinct vacuole system exists primarily in EC. Particle internalization may also occur via specific receptors (e.g. low-density lipoprotein/LDL-receptor, platelet-derived growth factor/PDGF-receptor, albumin-receptor) since nanoparticles covered with LDL (27), PDGF (28), and bovine serum albumin (29) have been shown to be internalized by cells via coated pits/vesicles. This might be of relevance since it is assumed that nanoparticles distributed in the blood stream are covered by specific protein subsets dependent on the physicochemical characteristics of the particles (30, 31). However, since the particle exposure *in vitro* was under static conditions, whereas the particle exposure *in vivo* is under floating and shear conditions, the way of particle internalization *in vivo* remains unclear.

Cytotoxicity and oxidative stress

Co and Ni nanoparticles induced a significant, concentration dependent impairment of cellular viability. In addition, we compared the effects of the nanoparticles with the effects of the metal ions Co^{2+} and Ni^{2+} (as chloride salts) in concentrations similar to the solid matter utilized. We observed that the particles exerted a higher cytotoxic effect than the corresponding ions. Thus, whereas a Co^{2+} concentration of 1 mM induced a reduction in cell number of ca. 20% after 24 h, Co particles induced a cell number reduction of about 35% at a concentration of ca. 0.85 mM. These findings were in agreement with the results of a study on the cytotoxicity of Co nanoparticles and Co^{2+} ions in mouse fibroblast Balb/3T3 cells (32).

At present we can only speculate about the higher cytotoxicity of transition metal nanoparticles compared to the corresponding metal ions. Severe problems may be due to the development of free radicals or ROS, which have been shown to be released by both transition metal ions (33-34) and (nano-)particles (5, 35). In addition, it has been shown that nanoparticles together with transition metals induce ROS production which exhibits a synergistic effect of nanoparticles together with transition metals (36). Since the nanoparticles used in this study exhibit a combination of both of these characteristics, i.e. nano-scaled particles composed of transition metals, a similar synergistic mechanism can be suggested.

The results from the DCDHF-DA assay showed a significant development of ROS by Co compounds. The effects were more pronounced for Co particles than for Co^{2+} ions and in contrast to Co^{2+} ions, Co particles showed a concentration-dependent increase in ROS amount. The GSH levels after 24 h exposure to Co compounds reflected the induction of oxidative stress as shown by the DCDHF-DA assay: A reduction of 40% occurred for both particle concentrations and the Co^{2+} treatment induced a reduction of the GSH content of about 30% for both concentrations. The intracellular depletion

of GSH stores is a sign for persisting oxidative stress. GSH plays a critical role in maintaining the intracellular redox balance and regulating oxidative stress signaling pathways, thus protecting cells from many forms of stress. The depletion of GSH has been linked to the pathophysiology of many diseases (37). The development of ROS by Co metal and Co^{2+} ions in the presence of superoxide dismutase and endogenous chelators like GSH is by a Fenton-like reaction (38-39). Transfer of one electron to O_2 results in the production of superoxide anion radicals, which can further give rise to the formation of other ROS (40). Thus, the reactions of Co metals and Co ions are capable of generating a whole spectrum of reactive oxygen species (39).

In contrast to the effects of Co compounds, both Ni compounds did not show any effect on DCF-fluorescence after 4 h. However, the GSH depletion of approximately 40% after 24 h Ni compound exposure compared to the untreated control indicated a persistent oxidative stress. At first, these contradictory results regarding ROS-development with different detector molecules are surprising. However, first of all, another time frame is observed by the different detector molecules and, secondly, it is known that DCDHF-DA-oxidation can compete with enzymatic ROS decomposition, and GSH is also an alternative target for ROS instead of DCDHF-DA (41). In conclusion, all compounds tested induced ROS-development. However, there is evidence that differences in the extent and characteristics occurred.

Pro-inflammatory activation

A pro-inflammatory effect in HDMEC occurred after exposure to both nanoparticle types. However, this pro-inflammatory induction was inconsistent in that a differential regulation of the tested pro-inflammatory factors occurred: 1) an enhanced release of IL-8 induced by both nanoparticle types; 2) ICAM-1 protein expression was enhanced by high amounts of Co particles, whereas Ni particles induced no distinct protein expression of ICAM-1; 3) a minor, concentration-dependent induction of MCP-1 release occurred after exposure to Co particles; Ni particles induced an inconsistent effect on MCP-1 release. In contrast to the particles, Co^{2+} and Ni^{2+} ions induced the expression of all pro-inflammatory markers tested (i.e. IL-8, MCP-1, ICAM-1).

The observed pro-inflammatory activation after Co particle exposure may be attributed to a release of Co^{2+} ions by corrosion of the particles, since the exposure of EC to these ions leads to impaired endothelial viability and pro-inflammatory stimulation (42). That Co^{2+} ions induce a concerted activation of the above mentioned transcription factors NF-κB and AP-1 has been demonstrated (43) and the Co particles used in this study induced pro-inflammatory activation comparable to that of Co^{2+} ions.

This contrasted with the effects of the Ni particles. Ni^{2+} ions induced an increase in the release of pro-inflammatory factors and the protein expression of endothelial cell adhesion molecules (i.e. ICAM-1), whereas Ni particles induced an increase in IL-8 release, without inducing a distinct expression of adhesion molecules. Thus, the possibility that Ni^{2+} ion release by the particles resulted in an induced pro-inflammatory stimulation was not supported by the pro-inflammatory effects induced by the respective ions. This indicated an activation mechanism by Ni particles that deviated from Ni^{2+} ion-induced activation shown to occur via a cooperation of the above-mentioned transcription factors NF-κB and AP-1 (43). Such differential activation of IL-8 and ICAM-1 was also shown by the treatment of endothelial and epithelial cells with H_2O_2 (44-45). Whereas H_2O_2 induced an IL-8 expression in epithelial cell lines without the expression of ICAM-1, EC expressed ICAM-1 after H_2O_2-treatment without the expression of IL-8. There is evidence that this cell type-specific, differential induction of IL-8 gene expression by H_2O_2 (and thus induced ROS) is by a differential binding of NF-κB and AP-1 to the IL-8 promoter (45). Since oxidative stress is also a relevant aspect in the mechanisms of (Ni) particulate matter-induced effects (5) such a differential activation of pro-inflammatory gene promoters may occur (46).

In conclusion this study shows that nanoparticles exert effects that deviate from those of possible corrosion products. However, whether the described effects shown *in vitro* are of relevance *in vivo* remains to be determined. Although much progress has been made within the last years to understand the effects of nanoparticles, knowledge about its

risk in humans is limited. This limitation is due to the complexity of the chemical and physical characteristics of nanoparticles in their interaction with the complex biology of human organisms. Thus, recent publications and the results of this study indicate that the toxicology of nanoparticles has more facets than anticipated so far and thus may comprise a risk of unforeseen effects to human health.

ACKNOWLEDGEMENTS

This work was supported by the Deutsche Forschungsgemeinschaft (Priority Programme Biosystem 322 1100, KI 601/1-4) and the European Commission (QOL-2002-147). The authors wish to thank Susanne Barth, Andrea Kölzow, Marianne Müller and Karin Molter for their excellent technical assistance.

REFERENCES

1. **Lomer M.C., R.P. Thompson, J. Commisso, C.L. Keen and J.J. Powell.** 2000. Determination of titanium dioxide in foods using inductively coupled plasma optical emission spectrometry. *Analyst 125: 2339.*
2. **Urban R.M., J.J. Jacobs, M.J. Tomlinson, J. Gavrilovic, J. Black and M. Peoc'h.** 2000. Dissemination of wear particles to the liver, spleen, and abdominal lymph nodes of patients with hip or knee replacement. *J. Bone Joint Surg. Am. 82:457.*
3. **Oberdorster G., E. Oberdorster and J. Oberdorster.** 2005. Nanotoxicology: an emerging discipline evolving from studies of ultrafine particles. *Environ. Health Perspect. 113:823.*
4. **Pope C.A., 3rd.** 2000. Epidemiology of fine particulate air pollution and human health: biologic mechanisms and who's at risk? *Environ. Health Perspect. 108(S):713.*
5. **Dick C.A., D.M. Brown, K. Donaldson and V. Stone.** 2003. The role of free radicals in the toxic and inflammatory effects of four different ultrafine particle types. *Inhal. Toxicol. 15:39.*
6. **Monteiller C., L. Tran, W. Macnee, S.P. Faux, A.D. Jones, B.G. Miller and K. Donaldson.** 2007. The pro-inflammatory effects of low solubility low toxicity particles, nanoparticles and fine particles, on epithelial cells *in vitro*: the role of surface area. *Occup. Environ. Med.* (electronically published ahead of print)
7. **Duffin R., A. Clouter, D.M. Brown, C.L. Tran, W. MacNee, V. Stone and K. Donaldson.** 2002. The importance of surface area and specific reactivity in the acute pulmonary inflammatory response to particles. *Ann. Occup. Hyg. 46(S):242.*
8. **Davies K.J.** 2000. Oxidative stress, antioxidant defenses, and damage removal, repair, and replacement systems. *IUBMB Life 50:279.*
9. **Frampton M.W., M.J. Utell, W. Zareba, G. Oberdorster, C. Cox, L.S. Huang, P.E. Morrow, F.E. Lee, D. Chalupa, L.M. Frasier, D.M. Speers and J. Stewart.** 2004. Effects of exposure to ultrafine carbon particles in healthy subjects and subjects with asthma. *Res. Rep. Health Eff. Inst. 126:1.*
10. **Takenaka S., E. Karg, C. Roth, H. Schulz, A. Ziesenis, U. Heinzmann, P. Schramel and J. Heyder.** 2001. Pulmonary and systemic distribution of inhaled ultrafine silver particles in rats. *Environ. Health Perspect. 109(S):547.*
11. **Geiser M., B. Rothen-Rutishauser, N. Kapp, S. Schurch, W. Kreyling, H. Schulz, M. Semmler, V. Im Hof, J. Heyder and P. Gehr.** 2005. Ultrafine particles cross cellular membranes by non-phagocytic mechanisms in lungs and in cultured cells. *Environ. Health Perspect. 113:1555.*
12. **Nurkiewicz T.R., D.W. Porter, M. Barger, L. Millecchia, K.M. Rao, P.J. Marvar, A.F. Hubbs, V. Castranova and M.A. Boegehold.** 2006. Systemic microvascular dysfunction and inflammation after pulmonary particulate matter exposure. *Environ. Health Perspect. 114:412.*
13. **Montgomery K.F., L. Osborn, C. Hession, R. Tizard, D. Goff, C. Vassallo, P.I. Tarr, K. Bomsztyk, R. Lobb, J.M. Harlan, et al.** 1991. Activation of endothelial-leukocyte adhesion molecule 1 (ELAM-1) gene transcription. *Proc. Natl. Acad. Sci. USA 88:6523.*
14. **Mukaida N., S. Okamoto, Y. Ishikawa and K. Matsushima.** 1994. Molecular mechanism of interleukin-8 gene expression. *J. Leukoc. Biol. 56: 554.*
15. **Roebuck K.A., A. Rahman, V. Lakshminarayanan, K. Janakidevi and A.B. Malik.** 1995. H2O2 and

tumor necrosis factor-alpha activate intercellular adhesion molecule 1 (ICAM-1) gene transcription through distinct cis-regulatory elements within the ICAM-1 promoter. *J. Biol. Chem. 270:18966.*

16. **Muller J.M., R.A. Rupec and P.A. Baeuerle.** 1997. Study of gene regulation by NF-kappa B and AP-1 in response to reactive oxygen intermediates. *Methods 11:301.*
17. **Peters K., H. Schmidt, R.E. Unger, M. Otto, G. Kamp and C.J. Kirkpatrick.** 2002. Software-supported image quantification of angiogenesis in an *in vitro* culture system: application to studies of biocompatibility. *Biomaterials 23:3413.*
18. **Gillies R.J. and D.W. Deamer.** 1979. Intracellular pH: Methods and applications. *Curr. Top. Bioenerg. 9:63.*
19. **Gillies R.J., N. Didier and M. Denton.** 1986. Determination of cell number in monolayer cultures. *Anal. Biochem. 159:109.*
20. **van Kooten T.G., C.L. Klein, M. Wagner and C.J. Kirkpatrick.** 1999. Focal adhesions and assessment of cytotoxicity. *J. Biomed. Mater. Res. 46:33.*
21. **LeBel C.P., H. Ischiropoulos and S.C. Bondy.** 1992. Evaluation of the probe 2',7'-dichlorofluorescin as an indicator of reactive oxygen species formation and oxidative stress. *Chem. Res. Toxicol. 5:227.*
22. **Bradford M.M.** 1976. A rapid and sensitive method for the quantitation of microgram quantities of protein utilizing the principle of protein-dye binding. *Anal. Biochem. 72:248.*
23. **Davda J. and V. Labhasetwar.** 2002. Characterization of nanoparticle uptake by endothelial cells. *Int. J. Pharm. 233:51.*
24. **Garcia-Garcia E., K. Andrieux, S. Gil, H.R. Kim, T. Le Doan, D. Desmaele, J. d'Angelo, F. Taran, D. Georgin and P. Couvreur.** 2005. A methodology to study intracellular distribution of nanoparticles in brain endothelial cells. *Int. J. Pharm. 298:310.*
25. **Peters K., R.E. Unger, C.J. Kirkpatrick, A.M. Gatti and E. Monari.** 2004. Effects of nano-scaled particles on endothelial cell function *in vitro*: studies on viability, proliferation and inflammation. *J. Mater. Sci. Mater. Med. 15:321.*
26. **Feng D., J.A. Nagy, H.F. Dvorak and A.M. Dvorak.** 2002. Ultrastructural studies define soluble macromolecular, particulate, and cellular transendothelial cell pathways in venules, lymphatic vessels, and tumor-associated microvessels in man and animals. *Microsc. Res. Tech. 57:289.*
27. **Handley D.A., C.M. Arbeeny and S. Chien.** 1983. Sinusoidal endothelial endocytosis of low density lipoprotein-gold conjugates in perfused livers of ethinyl-estradiol treated rats. *Eur. J. Cell Biol. 30: 266.*
28. **Rosenfeld M.E., D.F. Bowen-Pope and R. Ross.** 1984. Platelet-derived growth factor: morphologic and biochemical studies of binding, internalization, and degradation. *J. Cell. Physiol. 121:263.*
29. **Geoffroy J.S. and R.P. Becker.** 1984. Endocytosis by endothelial phagocytes: uptake of bovine serum albumin-gold conjugates in bone marrow. *J. Ultrastruct. Res. 89:223.*
30. **Blunk T., D.F. Hochstrasser, J.C. Sanchez, B.W. Muller and R.H. Muller.** 1993. Colloidal carriers for intravenous drug targeting: plasma protein adsorption patterns on surface-modified latex particles evaluated by two-dimensional polyacrylamide gel electrophoresis. *Electrophoresis 14:1382.*
31. **Luck M., B.R. Paulke, W. Schroder, T. Blunk and R.H. Muller.** 1998. Analysis of plasma protein adsorption on polymeric nanoparticles with different surface characteristics. *J. Biomed. Mater. Res. 39:478.*
32. **Sabbioni E., A.M. Gatti and T. Hartung.** 2004. Emerging disciplines in environmental pathology: part 2. *Pathol. Int. 54:141.*
33. **Ginsburg I., M. Sadovnic, J. Varani, O. Tirosh and R. Kohen.** 1999. Hemolysis of human red blood cells induced by the combination of diethyldithiocarbamate (DDC) and divalent metals: modulation by anaerobiosis, certain antioxidants and oxidants. *Free Radic. Res. 31:79.*
34. **Stohs S.J. and D. Bagchi.** 1995. Oxidative mechanisms in the toxicity of metal ions. *Free Radic. Biol. Med. 18:321.*
35. **Donaldson K., P.H. Beswick and P.S. Gilmour.** 1996. Free radical activity associated with the surface of particles: a unifying factor in determining biological activity? *Toxicol. Lett. 88:293.*
36. **Wilson M.R., J.H. Lightbody, K. Donaldson, J. Sales and V. Stone.** 2002. Interactions between ultrafine particles and transition metals *in vivo* and *in*

vitro. Toxicol. Appl. Pharmacol. 184:172.

37. **Winyard P.G., C.J. Moody and C. Jacob.** 2005. Oxidative activation of antioxidant defence. *Trends Biochem. Sci. 30:453.*
38. **Hanna P.M., M.B. Kadiiska and R.P. Mason.** 1992. Oxygen-derived free radical and active oxygen complex formation from cobalt(II) chelates *in vitro*. *Chem. Res. Toxicol. 5:109.*
39. **Leonard S., P.M. Gannett, Y. Rojanasakul, D. Schwegler-Berry, V. Castranova, V. Vallyathan and X. Shi.** 1998. Cobalt-mediated generation of reactive oxygen species and its possible mechanism. *J. Inorg. Biochem. 70:239.*
40. **Gilbert D.L.** 2000. Fifty years of radical ideas. *Ann. NY Acad. Sci. 899:1.*
41. **Jakubowski W. and G. Bartosz.** 2000. 2,7-dichlorofluorescin oxidation and reactive oxygen species: what does it measure? *Cell Biol. Int. 24:757.*
42. **Kirkpatrick C.J., S. Barth, T. Gerdes, V. Krump-Konvalinkova and K. Peters.** 2002. [Pathomechanisms of impaired wound healing by metallic corrosion products]. *Mund Kiefer Gesichtschir. 6:183.*
43. **Wagner M., C.L. Klein, T.G. van Kooten and C.J. Kirkpatrick.** 1998. Mechanisms of cell activation by heavy metal ions. *J. Biomed. Mater. Res. 42:443.*
44. **Lakshminarayanan V., D.W. Beno, R.H. Costa and K.A. Roebuck.** 1997. Differential regulation of interleukin-8 and intercellular adhesion molecule-1 by H2O2 and tumor necrosis factor-alpha in endothelial and epithelial cells. *J. Biol. Chem. 272: 32910.*
45. **Lakshminarayanan V., E.A. Drab-Weiss and K.A. Roebuck.** 1998. H2O2 and tumor necrosis factor-alpha induce differential binding of the redox-responsive transcription factors AP-1 and NF-kappaB to the interleukin-8 promoter in endothelial and epithelial cells. *J. Biol. Chem. 273:32670.*
46. **Peters K., R.E. Unger, A.M. Gatti, E. Sabbioni, E. Gambarelli and C.J. Kirkpatrick.** 2006. Impact of ceramic and metallic nano-scaled particles on endothelial cell functions *in vitro*. In *Nanomaterials - Toxicity, health and environmental issues.* C.S.S.R. Kumar ed. Wiley-VCH Weinheim, p. 108.